Journal of
Marine Science and Engineering

MDPI

Article

Structural Analysis Procedure and Applicability Review of Spudcan Considering Soil Types

Joo-Shin Park [1], Dong-Hun Lee [1] and Myung-Su Yi [2,*]

[1] Ship & Offshore Research Institute, Samsung Heavy Industries Co., Ltd., Geoje 53261, Republic of Korea
[2] Department of Naval Architecture and Ocean Engineering, Chosun University, Gwangju 61452, Republic of Korea
* Correspondence: true413@chosun.ac.kr; Tel.: +82-62-230-7182

Abstract: As interest in eco-friendly energy development continues to rise, the offshore wind turbine market is growing at a high rate of increase every year. In line with this, the demand for installation vessels with large capacity is also increasing rapidly. WTIVs (Wind Turbine Installation Vessels) employ spudcans in the seabed for the installation of wind turbines. Currently, the assessment of spudcans is an important issue in ensuring structural safety in the entire structure system. This study examines the current procedure suggested by classification societies and a new procedure that accounts for the new loading scenarios based on realistic operating conditions. This new procedure is further validated through an FEA (Finite Element Analysis). The current procedure yields maximum stress values below the allowable criteria because it does not consider the effect of the seabed slope, the leg bending moment, and the spudcan shape. However, the results of some load conditions as defined in the new procedure confirm the need for reinforcement under actual preload conditions. Therefore, the new procedure considers a broader range of real-world operating conditions, and the possible problems were verified through a detailed FEA.

Keywords: WTIV (Wind Turbine Installation Vessel); spudcan; structural strength estimation; preload condition; structural safety

check for updates

Citation: Park, J.-S.; Lee, D.-H.; Yi, M.-S. Structural Analysis Procedure and Applicability Review of Spudcan Considering Soil Types. *J. Mar. Sci. Eng.* **2023**, *11*, 1833. https://doi.org/10.3390/jmse11091833

Academic Editor: Liang Cui

Received: 28 August 2023
Revised: 17 September 2023
Accepted: 19 September 2023
Published: 20 September 2023

Copyright: © 2023 by the authors. Licensee MDPI, Basel, Switzerland. This article is an open access article distributed under the terms and conditions of the Creative Commons Attribution (CC BY) license (https://creativecommons.org/licenses/by/4.0/).

1. Introduction

The offshore wind power industry is growing rapidly based on continuous technology development, cost reduction, and supportive development policies. Considering that more than 70% of the Earth is covered by the sea, and that offshore wind speeds are stronger than those on land, the case for offshore wind power development is compelling. In terms of carbon reduction, 1 GW of offshore wind power stands out as a highly attractive alternative to fossil fuels rather than solar and hydropower because it prevents over 3.5 metric tons of carbon dioxide emissions. The global new offshore wind power market is expected to grow at an average annual rate of 23% until 2025, exceeding 20 GW in 2025 and reaching 32 GW in 2030. In particular, the new power generation market is expected to be led by Asia, with 52 GW in China, 10.5 GW in Taiwan, and 7.9 GW in Korea [1]. In response to these expanding development initiatives, expectations of orders for large-scale Wind Turbine Installation Vessels (WTIVs) are growing in the shipbuilding industry. According to Clarksons Research (a British shipbuilding and shipping market analysis agency), wind turbine capacity is projected to increase from 12 MW to 15 MW in the future, and a new cycle will come for large-scale WTIV orders. The core equipment that composes a WTIV is the jacking system that raises and lowers the legs and the crane that is used to install and dismantle the wind turbine.

The structural members of the WTIV can be divided into three main parts: legs, spudcans, and hull structures, as shown in Figure 1. Among them, the spudcan, positioned at the end of the leg, plays a key role in ensuring the stable operation of the WTIV by

anchoring the seabed upon arrival at the installation site. In general, a WTIV installs wind turbines in the order of tower, nacelle, and blade after the substructure is installed. The installation of one wind turbine takes approximately 12 to 15 h. The main components constituting the WTIV include the hull, legs, deck house, main crane, jack case, and helideck, as shown Figure 1. Among these, the leg and spudcan are the most critical components. The leg is fixed to the seabed when lifting the hull to install the wind turbine, playing an important role in ensuring safe operations. The shape and area of the spudcan must be well determined to ensure optimal load distribution during the preloading stage.

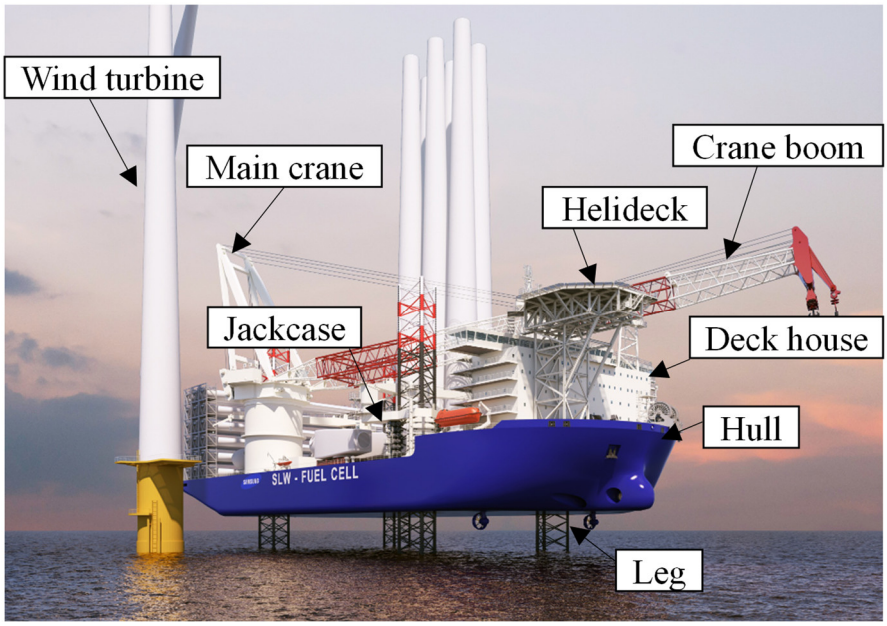

Figure 1. Naming of main components in the WTIV.

The purpose of this study is to take the safety of the spudcan to the next level by presenting a more reasonable structural safety evaluation method and criteria for the WTIV spudcans. A review of relevant prior studies reveals the following.

Osborne et al. [2] introduced the main results from the development of guidelines (InSafeJIP) for the integrated management of items arising from ground problems during jack-up rig operations. It is expected that the major points related to the new procedure proposed in the research will complement the points that have not been previously addressed in the past and improve the structural safety related to the installation and disassembly of the jack-up unit.

Puyang et al. [3] conducted a study on a numerical analytical method to predict the penetration depth in the preloading process of a jack-up rig. This method can consider the nonlinearity of the geological conditions, which is not considered in the existing empirical formulas, and the effect on the maximum soil bearing capacity and penetration depth was analyzed. Influencing factors were derived through numerical analysis of the main design variables, and a comparative evaluation was conducted using the geological conditions of the Bohai No. 5 platform to validate the assessment method. When compared with the existing empirical formula, the maximum soil bearing capacity and penetration depth matched well, and the numerical analysis method proposed in this study is expected to provide a more accurate prediction of penetration behavior.

Cho et al. [4] conducted a study on the development of the legs for a wind installation ship intended for use in a wind power demonstration complex in the Southwest Sea of Korea. Environmental load conditions and geological surveys in the vicinity of the wind farm were included to design a spudcan suitable for the marine environment. The stratum composition is mostly sand and clay, and it was confirmed that ground subsidence occurred in some sections. The representative geological stiffness from the southwestern sea was extracted and

used to evaluate the structural strength of the legs, and it was confirmed that about 20% of the structural strength margin was achieved compared to the existing pinned condition.

The leg structure of the WTIV is a pipe structure exposed to significant in-plane bending. Because the pipes in the leg structure are relatively long and thin, when modeled using 2D shell elements, an excessive number of elements are needed, and also it is difficult to expect accuracy in this analysis. Therefore, structural analysis using 1D beam elements has been mainly conducted so far. Recently, Fonseca and Meld [5] presented an alternative method that can replace finite shell elements and is attracting attention to overcome the shortcomings of existing structural analysis methods.

Jin et al. [6] performed spudcan shape analysis and structural design based on soil data obtained from surveys in the southwest coast. For the soil penetration analysis, a series analysis of the shape and area of the spudcan was performed using ABAQUS 2013, a commercial analysis program. To increase the ground bearing capacity of the spudcan, a rectangular shape was recommended rather than a circular shape, and a structural safety-oriented design incorporating spudcan penetration and a chord was proposed. The numerical analysis method and the Society of Naval Architects and Marine Engineers (SNAME) results showed similarities within a penetration depth of 10 m. Beyond this depth, the SNAME results tended to be conservative. As the main cause, the soil plug effect was analyzed. In particular, the prediction of the punch-through behavior that occurs in the combination of strong and weak geological layers showed similar results in both conditions.

Park et al. [7] studied the engineering procedures for the main core structures of the jack-up rig, specifically the leg, hull, and cantilever structures. It was emphasized that mutual data compatibility was essential for each evaluation order, and procedures were developed to conduct both global and local structure analyses using both 1D beam elements and 2D shell elements. Finally, a new procedure for the structural safety review for the preloading stage was proposed. The predicted spudcan penetration behavior and the value observed in the jack-up rig were similar to the high level of the calculated value, and the maximum load and penetration depth were quickly inferred by introducing an appropriate range of safety factors from the results of the existing empirical formula [8].

Yu et al. [9] conducted a numerical analysis using the Coupled Euleran–Lagrangian Method (CEL) to explore the impact of three different spudcan shapes in geological conditions where jack-up rigs are typically installed. As the slope depth of the support surface increases, spudcans with a flat bottom tended to increase the lateral load and moment a lot, and similar characteristics were confirmed in the inclined type and the model with a skirt. The authors argued that the structural strength should not be a problem as long as the results for the penetration analysis of the existing flat model considered seabed slopes or an existing penetration shape. They emphasized the need for a thorough review of the spudcan's shape regarding these factors.

Yu et al. [10] proposed to perform an optimizing study of the spudcan structures, and the effectiveness of them were analyzed. Firstly, 3D Large Deformation Finite Element (LDFE) Analyses were carried out using the Coupled Eulerian–Lagrangian (CEL) method in the commercial finite element package ABAQUS. After calibrating the validity of the numerical calculation model against existing centrifuge test data and LDFE results, the differences in the interaction mechanism between the novel spudcans and the generic spindle-shaped spudcan were studied when penetrating near an existing footprint with an eccentric distance of 0.5D. The horizontal range of plastic deformation of the disturbed soils, the inclination angle of the spudcan, and the offset distance of the pile legs were analyzed comparatively as well. The results show that the proposed novel spudcans can mitigate the maximum horizontal sliding force and the maximum bending moment at the top of the pile leg obviously, compared with those of the generic one, which were reduced by 32.59%, 22.47%, and 28.18% and 26.32%, 12.88%, and 18.02%, respectively.

Cassidy et al. [11] assessed the appropriate stiffness levels for a numerical simulation. Utilizing results from a detailed "pushover" experiment of a three-legged model jack-up on dense sand, the study compares the experimental pushover loads and displacements on

the hull and spudcans to numerical simulations using different assumptions of spudcan stiffness. These include pinned and encastré footings, linear springs, and a force-resultant model based on displacement-hardening plasticity theory. Constant stiffness levels are shown to be inadequate in simulating the experimental pushover test. The nonlinear degradation of stiffness associated with the latter force-resultant model is critical.

Previous studies focused on spudcan penetration behavior, with limited attention given to scenarios and detailed structural strength evaluation procedures based on load conditions. Therefore, an engineering procedure was newly developed considering real-world conditions that may occur in the spudcan structure used in WTIVs. The derived results were compared with the current procedure's methodology.

2. Spudcan Engineering

2.1. Preloading

After loading the wind turbine on the deck using a crane at the port, the WTIV moves to the installation area, as shown in Figure 2a. Upon arrival in the designated offshore location, the leg is lowered to the seabed, as shown Figure 2b. Penetration begins the moment the spudcan touches the seabed, as seen in Figure 2c. The hull is lifted out of the water surface using a jacking system to ensure that the spudcan is completely fixed on the seabed. At this time, the effect of buoyancy is reduced and ensures stable penetration. The penetration depth varies depending on the preloading value and the geologic characteristics of the seabed, ranging from 3 m for a typical sand layer to 5 m to 15 m for a clay layer, as shown in Figure 2d. In general, the geological survey results of the installation location are analyzed in advance to calculate the maximum penetration depth under the WTIV's lifting capacity, and vessel operations are based on this information. Table 1 lists the main specifications of the WTIV used in the study.

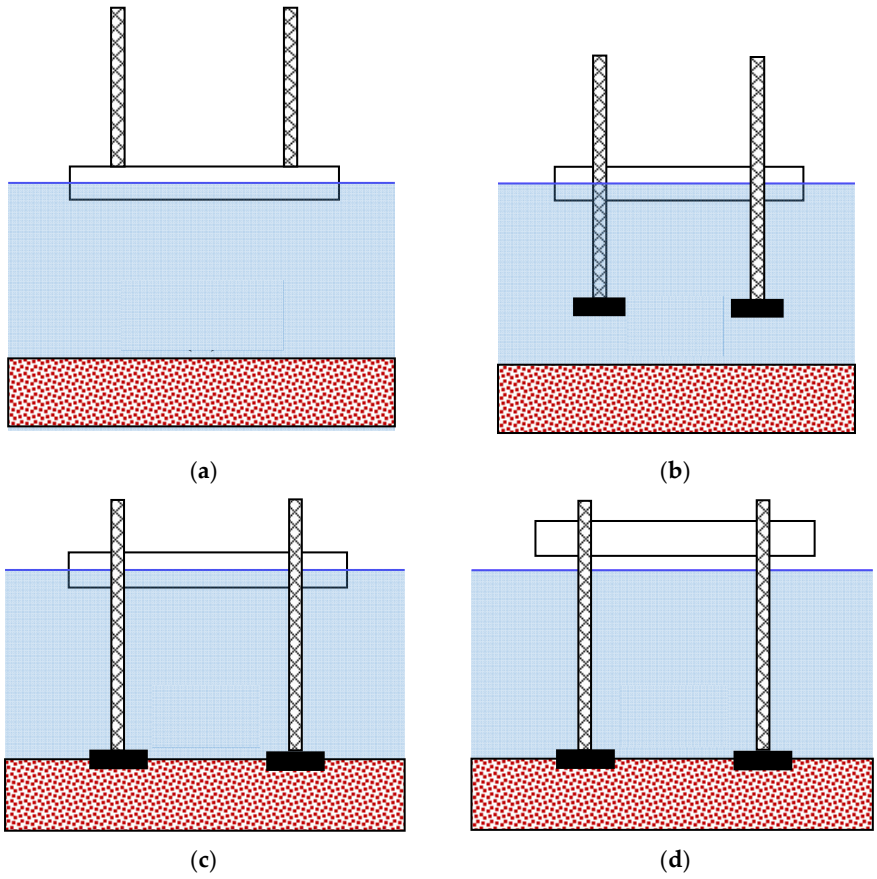

Figure 2. Preloading procedure: (**a**) transit, (**b**) leg lowering, (**c**) preloading, (**d**) elevating.

Table 1. Main dimensions of the target WTIV.

Item	Description
Length overall	160.0 m
Breadth overall	60.0 m
Depth, molded	13.0 m
Length of leg	110.0 m
Number of legs	4
Max. elevated weight	46,500 mt
Max. preload per leg	23,250 mt
Jacking capacity	41,000 mt
Max. water depth	75.0 m
Max. crane capacity	2500 mt
Max. penetration depth	3.0 m

2.2. Existing Spudcan Design Load and Evaluation Procedure

The procedure for the structural strength review of the spudcan is schematically shown in Figure 3, based on the Norwegian Classification Society [12] standard, which is the only standard mentioned for evaluating spudcan structural strength. Once the initial structural design is completed, the load conditions for structural strength evaluation are calculated. It is assumed that if the seabed is soft, such as a clay layer, the entire spudcan area comes into contact with the seabed, resulting in an even load distribution based on the spudcan's weight. In hard soil, it is recommended to consider only 50% of the spudcan's contact area. The hydrostatic pressure at the maximum sea depth where the WTIV is installed corresponds to the total area exposed to the seawater, and this condition is sufficiently negligible from a structural strength perspective.

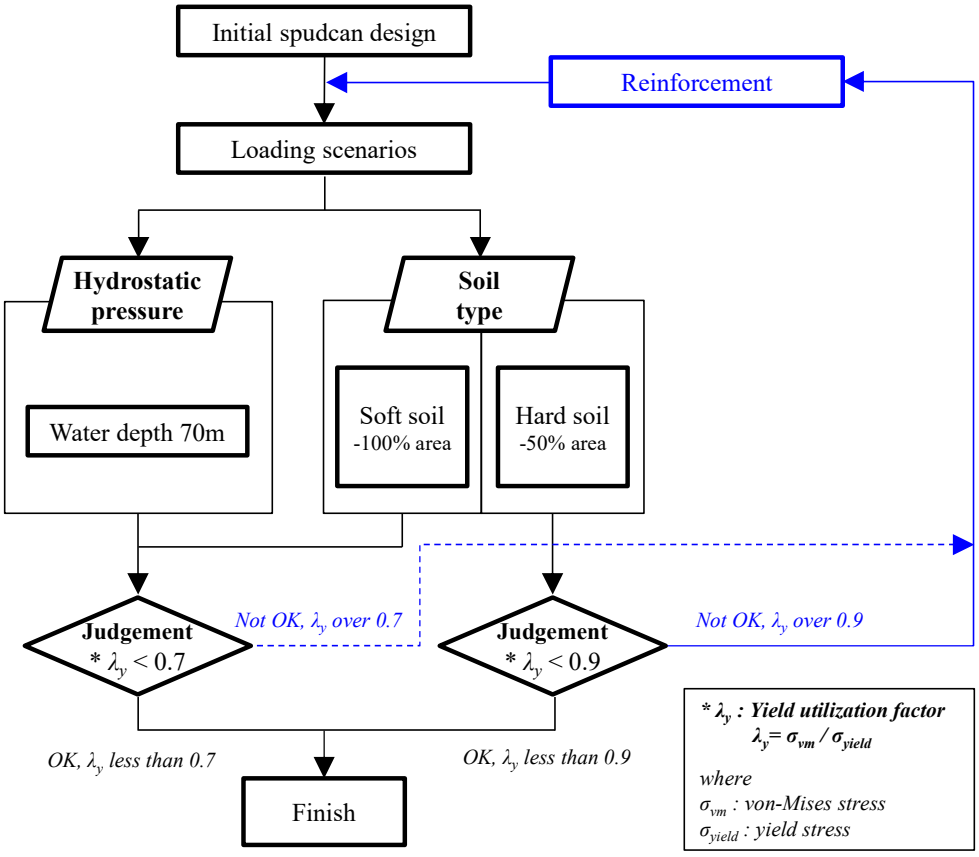

Figure 3. Current procedure for strength analysis of spudcans.

The safety factors mentioned in the classification criteria use 0.7 and 0.9, with 0.9 applied only when the contact area is 50%. The reason is that the maximum stress occurs in this condition, so a larger allowable safety factor is applied. If the allowable stress is not satisfied as a result of structural strength analysis, an iterative review is performed through structural reinforcement design.

The primary challenge with the currently used procedure is that it lacks consideration of more diverse conditions that may arise in hard soil conditions and that the technical basis for determining the load condition is inaccurate.

2.3. Improved Spudcan Design Loads and Evaluation Procedure

Figure 4 shows the improved spudcan structural strength evaluation procedure proposed in this study. The difference between the improved structural strength evaluation procedure and the existing procedure lies in the subdivision of the load conditions of the spudcan that can occur depending on the seabed conditions.

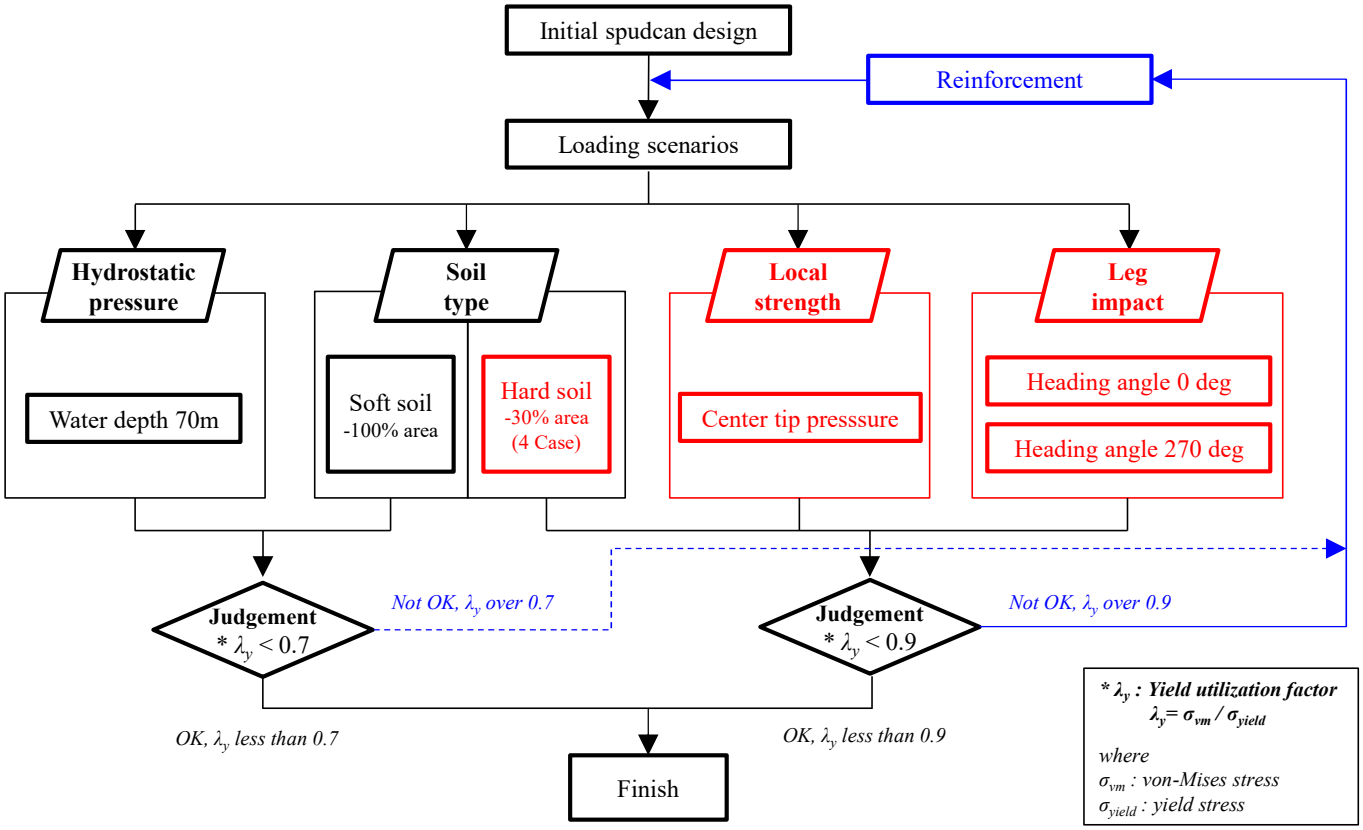

Figure 4. Newly proposed procedure for strength analysis of spudcans.

2.3.1. Contact Condition

As described above, in the existing spudcan structural strength evaluation procedure, the contact area is classified as 50% and 100% regardless of the seabed conditions, and there is no technical basis for this. Once a contract is signed with an offshore wind farm, the WTIV operators usually collect seabed data to estimate the maximum penetration depth under a full load. Determining the shape of the spudcan is crucial in the case of hard ground, as it must perform reliably across diverse sea areas and ground types. Considering the area of each component of the tetragonal spudcan with a diagonal slope considered in this study, it is reasonable to assume that the minimum contact area is 35%. In this case, the positioning of the contact area is designed to consider potential conditions while considering the symmetrical shape of the spudcan.

2.3.2. Local Strength

In scenarios where the spudcan penetrates hard soil, a local concentrated load may occur at the spudcan's tip during the initial stages. If structural damage occurs at the tip of the spudcan, proper penetration does not occur and rotation of the spudcan occurs, resulting in an asymmetrical pressure distribution. Therefore, in the improved evaluation procedure, the condition of applying a concentrated load equal to the preload to the tip of the spudcan as a design load was added to ensure the safety of the local structural strength of the spudcan.

2.3.3. Impact Load Intensity

During spudcan penetration, particularly on seabed slopes or areas with an existing footprint, as depicted in Figure 5, the spudcan's position can abruptly shift, resulting in impact loads on the side of the spudcan, which may pose a problem to the safety of the WTIV. The magnitude of the impact load on the side of the spudcan is determined by the maximum moment around the bottom of the lower guide including the hull structure.

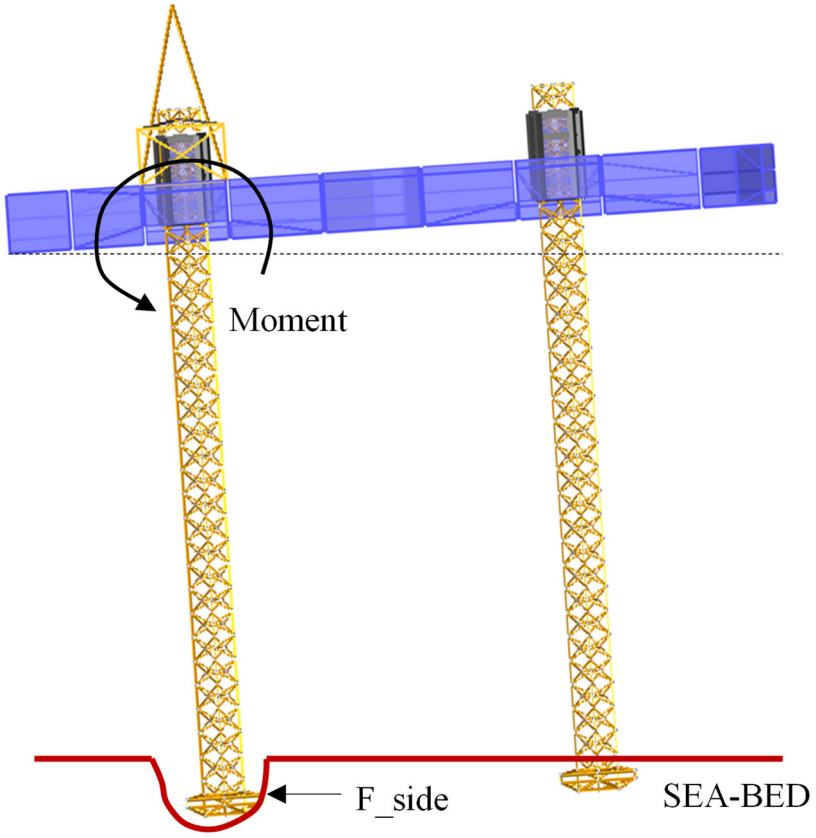

Figure 5. Asymmetric spudcan penetration and behavior.

The improved procedure includes a step of evaluating the strength check by applying a safety factor of 0.9 to the design load so that it can generate a moment of the same magnitude of the side force (F_side) at the spudcan's side, as shown in Figure 5.

3. Structural Strength Analysis and Results

In this study, the comparison of results obtained by applying a new procedure that introduces additional evaluation criteria to account for real-world behavior with the existing procedure used for assessing the structural strength of the spudcan will be presented. To verify the proposed new methodology, a numerical analysis program of MSC Patran/Nastran 2016 [13] was used to examine the structural safety of the spudcan. The Nastran solver was applied to evaluate the structural strength reflecting the structural shape of the leg

and spudcan connections. Although an advanced structural analysis method such as nonlinear analysis or dynamic structural analysis is required for an accurate result, it is not easy to perform a structural analysis at that level in the industrial field. Therefore, in this paper, a structure evaluation procedure using static structure analysis was developed to perform structure evaluation in the field. This static structure analysis was made possible by introducing a dynamic factor that could reflect dynamic effects to reflect load conditions, such as impact loads.

3.1. Analysis Model

The spudcan has a tetragonal shape and is designed to stably penetrate the slope of the seabed. The footing area is 200 m^2, and the tip area is 6.3 m^2. Figure 6 illustrates the spudcan structural analysis model. The analysis model was created with 21,655 nodes and 25,595 elements using 2D shell elements for plate members and 1D beam elements for stiffener members. About 95% of all 2D shell elements were generated using a quad mesh, and tri mesh was used for the other member.

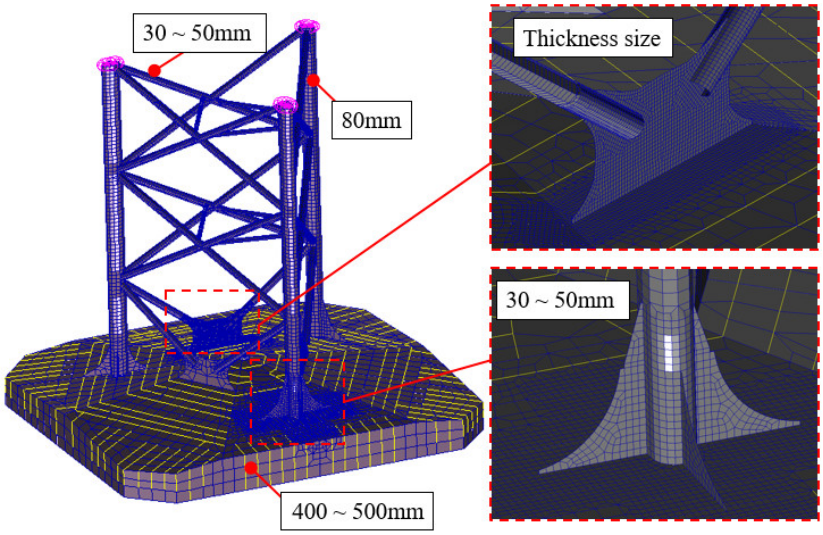

Figure 6. Mesh size according to members.

The mesh size was set so that the size of the member could be expressed without distortion, and the connection parts where the stress concentration occurred (leg–bracket, spudcan–gusset plate, and brace connection) had a mesh size of 50 mm or less. The leg chord is divided into about 80 mm, and the mesh size of a typical spudcan is less than 500 mm, as shown in Figure 6. The size of the elements recommended in structural strength analysis is the width between stiffeners, and in the case of hulls 800 mm is commonly used. However, the spudcan has a structural shape characteristic; therefore, there is a need to subdivide the size of the elements.

The installation ship is planning to operate at the North Sea offshore wind farm, where the seabed is composed of a dense sand layer. The maximum preload is determined as 50% of the maximum lifting weight, and the maximum penetration depth is determined based on this load. In this study, 23,250 tons were calculated, and the maximum penetration depth is 3 m under the mentioned conditions.

As there is no detailed procedure document related to the evaluation of the structural strength of the spudcan proposed by the classification society, and some of the conditions mentioned are ambiguous, real-world applications often face significant discrepancies. The spudcan, legs, and connecting brackets used in the analysis were modeled in detail, as shown Figure 7. Since the spudcan has a very complex grillage structure arrangement for good load transfer from the upper leg, the modeling accuracy plays a big role in evaluating structural safety.

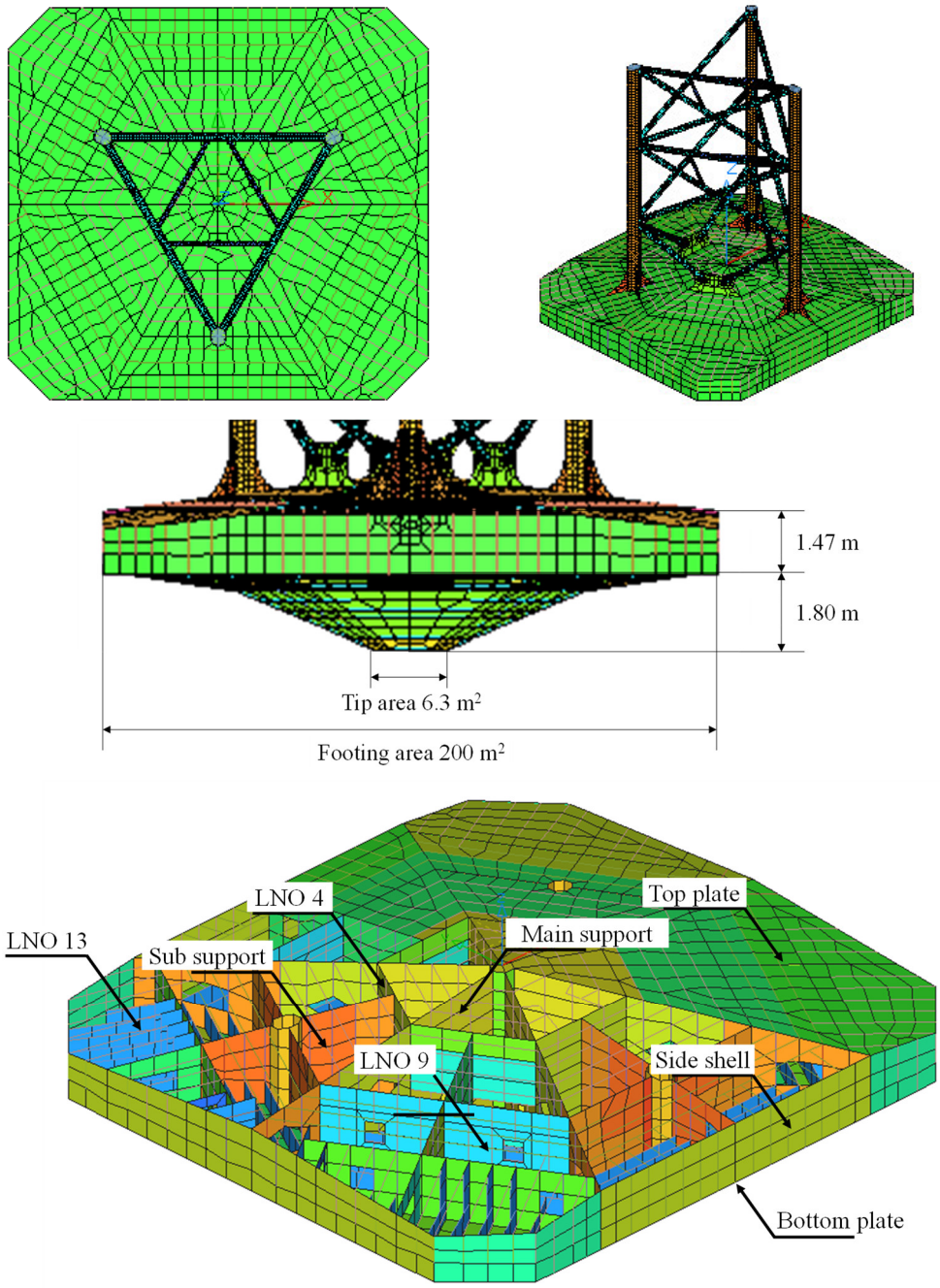

Figure 7. The finite element model of spudcan.

3.2. Analysis Conditions

Table 2 indicates the main dimensions of the target spudcan structure under study, and Table 3 presents the environmental load conditions during the preloading stage.

Table 2. Main dimension of the target spudcan.

Item	Description
Footing area	200.0 m^2
Tip area	6.3 m^2
Penetration depth	3.0 m
Height (bottom–top line)	3.27 m
Shape	Tetragon

Table 3. Design data under preload condition.

Item	Description
Water depth	70.0 m
Air gap	15.0 m
Max. wave height	7.5 m
Wave period	12.9 s
Wind speed	25.0 m/s
Current speed	1.2 m/s

For the wave period, wind speed, and current speed, the design conditions were selected by referring to the 100-year return period marine data from the North Sea. The WTIV can load five units (tower, nacelle, and blade) of 12 MW turbines on the main deck, with a maximum lifting weight of 46,500 tons. During wind turbine installation, when fixing the spudcan through seabed penetration, preloading is performed by alternating between two legs. In the analysis, the maximum penetration weight per spudcan was limited to 23,250 tons.

3.3. Boundary Conditions and Design Load Conditions

For the analysis, the upper end of the leg was fixed as the boundary condition. The load conditions according to the procedure can be classified into Tables 4 and 5, and the load conditions of the newly proposed procedure are subdivided. Table 4 represents the required design load conditions within the existing spudcan structural evaluation procedure, and Table 5 represents the design load conditions in the improved evaluation procedure.

Table 4. Design load cases for the existing design procedure.

Load		Direction	Design Value			Applied Load		Safety Factor	Note
LC	Description		Vert. (MN)	Moment (MNm)	Hori. (MN)	Pressure (MPa)	Contact Area (m^2)		
LC01	Hydrostatic pressure	-	-	-	-	0.70 [(2)]	-	1.43	Water depth 70 m
LC02	Preload on soft soil	-	228 [(1)]	-	-	1.14	200	1.43	Elevated weight 23,250 ton
LC03	Preload on hard soil	Centric	228 [(1)]	-	-	2.28	100	1.11	Contact area = 0.5 × Full area
LC04	Preload on hard soil	30°	228 [(1)]	-	-	2.28	100	1.11	
LC05	Preload on hard soil	60°	228 [(1)]	-	-	2.28	100	1.11	
LC06	Preload on hard soil	270°	228 [(1)]	-	-	2.28	100	1.11	

Note: [(1)] 228 MN = 23,250 ton (Elevated weight) × 9.81 m/s^2. [(2)] 0.70 MPa = 1025 kg/m^3 × 9.81 m/s^2 × 70 m (Water depth) × 10^{-6} m^2/mm^2.

Table 5. Design load cases for the newly proposed procedure.

Load		Direction	Design Value			Applied Load		Safety Factor	Note
LC	Description		Vert. (MN)	Moment (MNm)	Hori. (MN)	Pressure (MPa)	Contact Area (m^2)		
LC01	Hydrostatic pressure	-	-	-	-	0.70 [(2)]	-	1.43	Water depth 70 m
LC02	Preload on soft soil	-	228 [(1)]	-	-	1.14	200	1.43	Elevated weight 23,250 ton
LC03	Preload on hard soil	Centric	228 [(1)]	-	-	3.80	60	1.11	Contact area = 0.3 × Full area
LC04	Preload on hard soil	30°	228 [(1)]	-	-	3.80	60	1.11	
LC05	Preload on hard soil	60°	228 [(1)]	-	-	3.80	60	1.11	
LC06	Preload on hard soil	270°	228 [(1)]	-	-	3.80	60	1.11	
LC07	Local tip load	-	228 [(1)]	-	-	36.2	6.3	1.11	
LC08	Leg impact	0°	-	133.6	7.71 [(3)]	0.57	13.6	1.11	Water depth 25 m, Dynamic factor 1.3
LC09	Leg impact	90°	-	133.6	7.71 [(3)]	0.57	13.6	1.11	

Note: [(1)] 228 MN = 23,250 ton (Elevated weight) × 9.81 m/s^2. [(2)] 0.70 MPa = 1025 kg/m^3 × 9.81 m/s^2 × 70 m (Water depth) × 10^{-6} m^2/mm^2. [(3)] 7.71 MN = 133.6 MNm/25 m × 1.3.

3.3.1. Hydrostatic Loading

The hydrostatic load is applied to the exposed top surface of the spudcan, as shown in Figure 8, with the hydrostatic pressure at the maximum depth of 70 m under the analysis conditions. The bottom surface in contact with the seabed is subjected to a translational motion fixing condition. The conditions for the application of the improved evaluation procedure are the same as the original evaluation procedure. This application condition remains the same for both the existing procedure and the improved procedure.

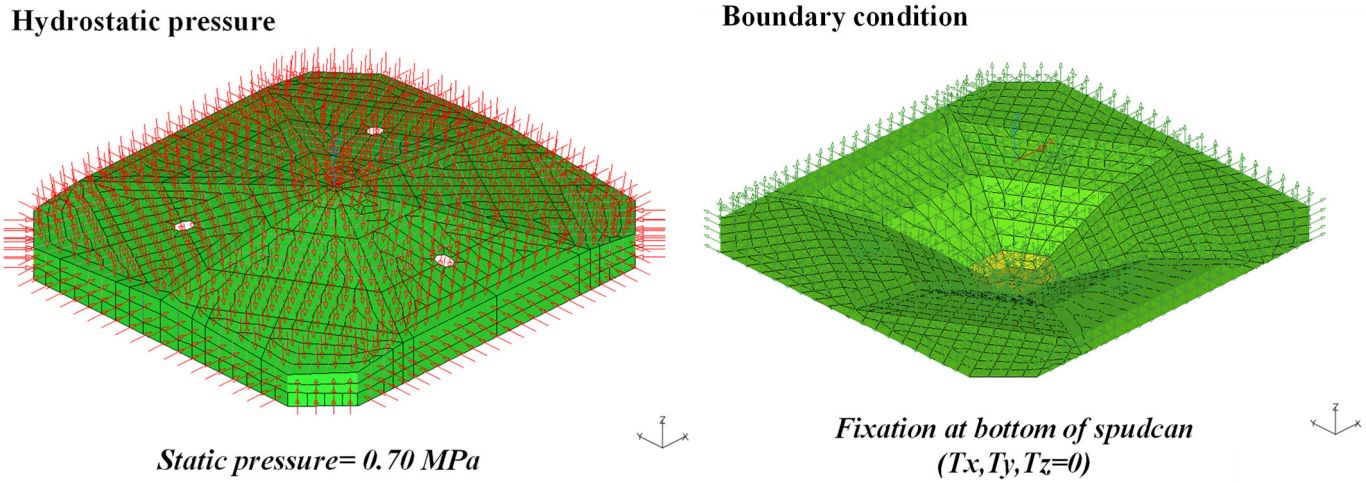

Figure 8. Application of hydrostatic pressure (LC01).

3.3.2. Soil Bearing Capacity

The ground support condition is the support force generated by the preload due to the contact of the lower surface of the spudcan with the seabed and is considered separately for

soft soil conditions such as a clay layer and hard soil conditions such as sheet sand. For the boundary condition, a fixed condition is applied at the end of the leg, as shown in Figure 9.

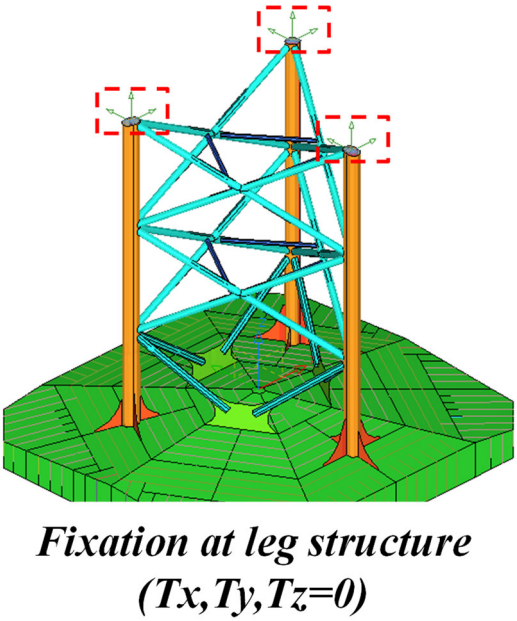

Figure 9. Boundary conditions.

For soft soil conditions, the soil bearing capacity is distributed over the entire area of the spudcan, and it is realized in the Finite Element Analysis, as shown in Figure 10. It applies equally to both the existing and improved procedures.

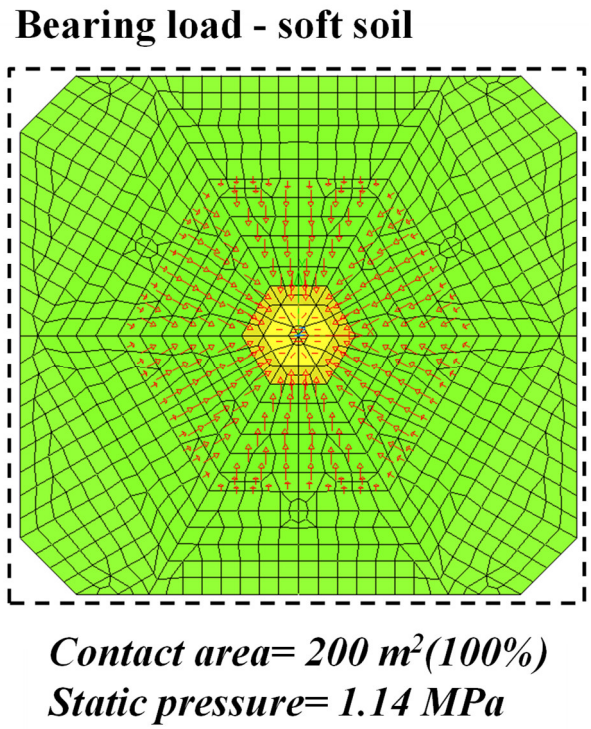

Figure 10. Application of vertical bearing load for soft soil condition (LC02).

In hard soil conditions, the existing procedure implements bearing capacity by entering a static pressure so that the preload acts on a contact area of 50% of the total area. The improved procedure considers a contact area of 30% of the total area and is applied as

shown in Figure 11. Considering the symmetry of the tetragonal structure of the spudcan, a total of four contact area conditions were applied in consideration of the symmetry of the tetragonal structure of the spudcan, which is the subject of this study.

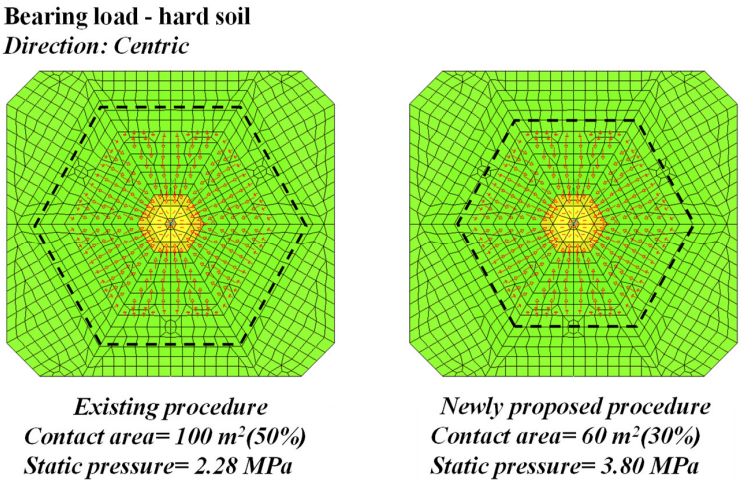

(**a**)

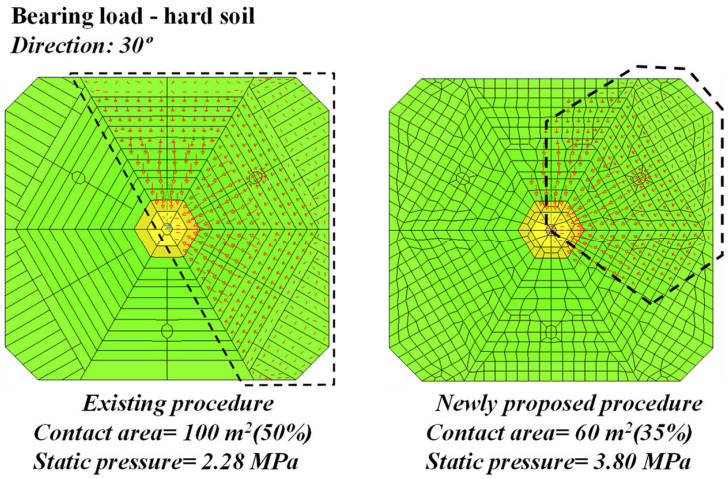

(**b**)

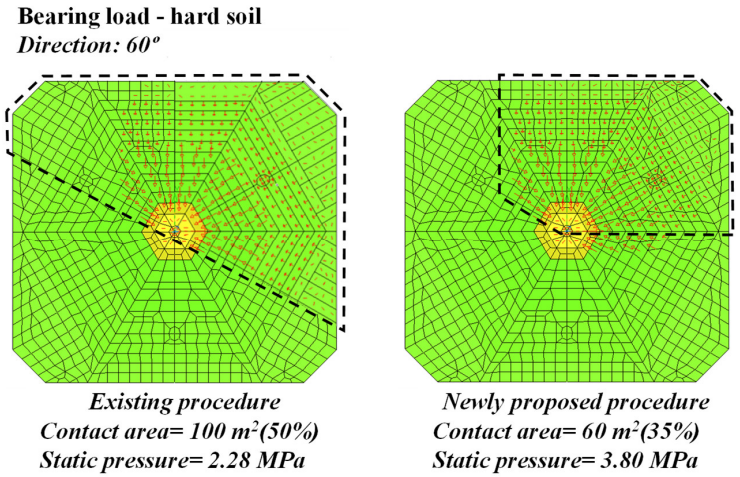

(**c**)

Figure 11. *Cont.*

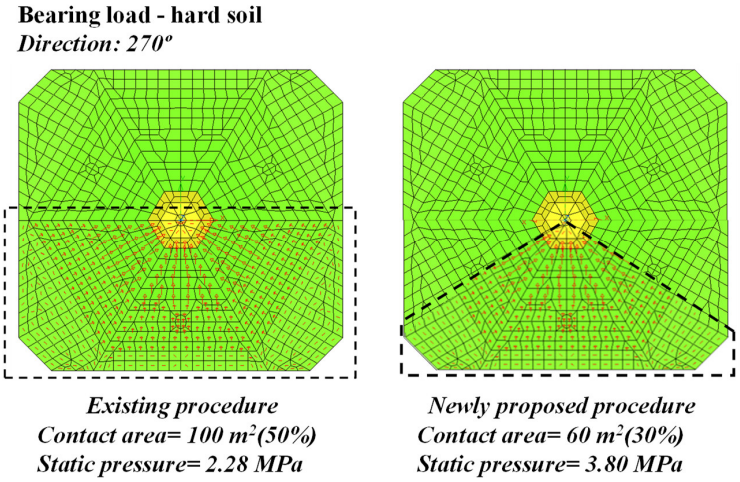

(**d**)

Figure 11. Applications of vertical bearing load for hard soil condition: (**a**) load direction/centric (LC03); (**b**) load direction/0 deg. (LC04); (**c**) load direction/30 deg. (LC05); (**d**) load direction/270 deg. (LC06).

3.3.3. Local Reaction Force

In the improved procedure, the load acting on the tip of the spudcan during the initial stage of penetration in hard soil is represented in the Finite Element Analysis as a localized pressure by dividing the preload by the tip area, as shown in Figure 12.

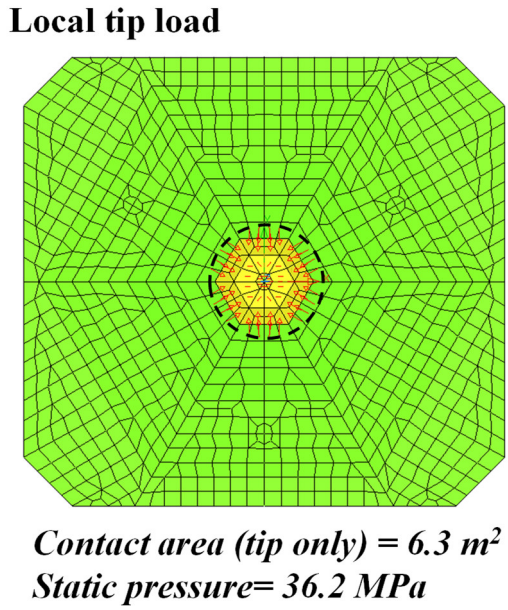

Figure 12. Applications of local tip load (LC07).

3.3.4. Horizontal Leg Impact Load

As previously mentioned, the impact load of the spudcan must be reflected on the side of the spudcan by calculating the appropriate lateral load to apply a moment on the spudcan with the same size as the moment generated by the lower guide where the leg and the leading angle meet. In this study, the maximum bending moment of the lower guide obtained through the wire analysis of the WTIV was used to calculate the lateral load, as shown in Equation (1). The length of the moment arm at this time is equal to the

water depth. A dynamic factor of 1.3 [14] was applied to consider the dynamic effect of the impact load.

$$Leg\ impact\ load = Moment\ at\ lower\ guide \div Water\ depth \times Dynamic\ factor \quad (1)$$

The location where the lateral load acts should be determined by considering the shape, symmetry, and possible eccentric load directions of the spudcan. Figure 13 presents the location of the lateral impact load applied in this study, along with the corresponding boundary conditions at that time.

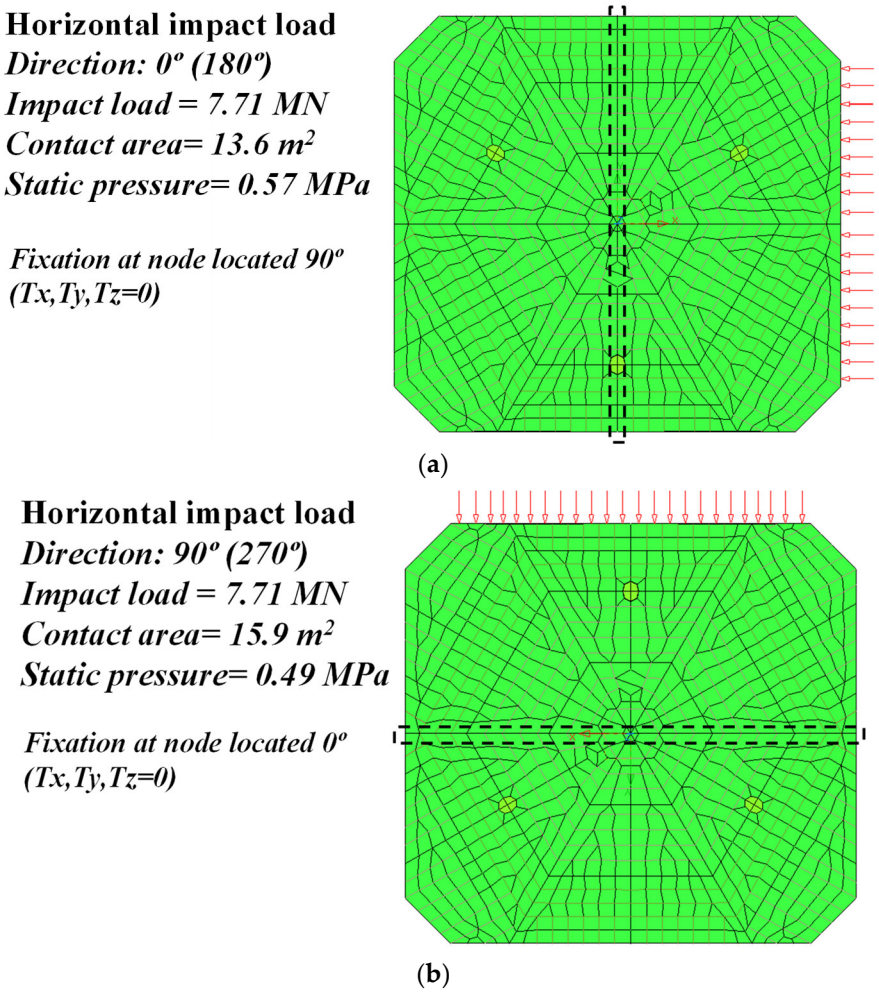

Figure 13. Applications of horizontal leg impact load: (**a**) load direction 0 deg. (180 deg.) (LC08); (**b**) load direction 90 deg. (270 deg.) (LC09).

3.4. Analysis Results

3.4.1. Structural Strength Assessment

To compare the differences in the structural members according to the structural safety review procedure of the spudcan, the structure of the spudcan that satisfies the allowable conditions was derived using only the plate thickness while keeping the structure shape in Figure 14. The stress difference in the top plan is the largest, and in order to reduce weight, steel with a yield stress of 690 MPa was applied to increase the range of allowable stress. The original spudcan has a yield stress of 355 MPa.

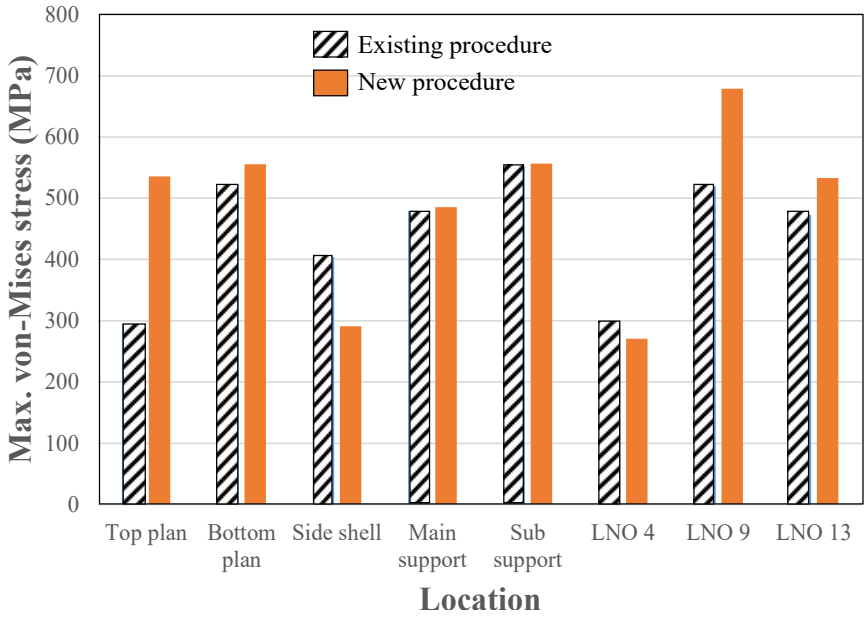

Figure 14. Comparison of the maximum von Mises stress between the existing procedure and the proposed procedure.

Table 6 indicates the maximum von Mises stress results and allowable stress values for each section of the spudcan structure using the existing procedure, while Table 7 shows the results using the improved procedure. Figure 14 illustrates the comparison result of the maximum von Mises stress. Figures 15 and 16 represent the von Mises stress distributions on the bottom surface and the outer ribs.

Table 6. Max. von Mises stress results of the spudcan based on the existing design procedure.

Location	Max. von Mises Stress (MPa)	Load Case No.	Description
Top plane	294.50	LC04	Preload_hard_30°
Bottom plane	521.98	LC06	Preload_hard_270°
Side shell	404.32	LC06	Preload_hard_270°
Main support	479.30	LC06	Preload_hard_270°
Sub support	552.67	LC06	Preload_hard_270°
LNO 4	297.42	LC04	Preload_hard_30°
LNO 9	519.52	LC06	Preload_hard_270°
LNO 13	472.94	LC04	Preload_hard_30°

Table 7. Max. von Mises stress results of the spudcan based on the newly proposed design procedure.

Location	Max. von Mises Stress (MPa)	Load Case No.	Description
Top plane	535.79	LC04	Preload_hard_30°
Bottom plane	534.55	LC07	Local tip load
	555.62	LC06	Preload_hard_270°
Side shell	290.99	LC04	Preload_hard_30°
Main support	485.69	LC05	Preload_hard_60°
Sub support	556.34	LC04	Preload_hard_30°
LNO 4	270.84	LC04	Preload_hard_30°
LNO 9	678.42	LC06	Preload_hard_270°
LNO 13	532.77	LC05	Preload_hard_60°

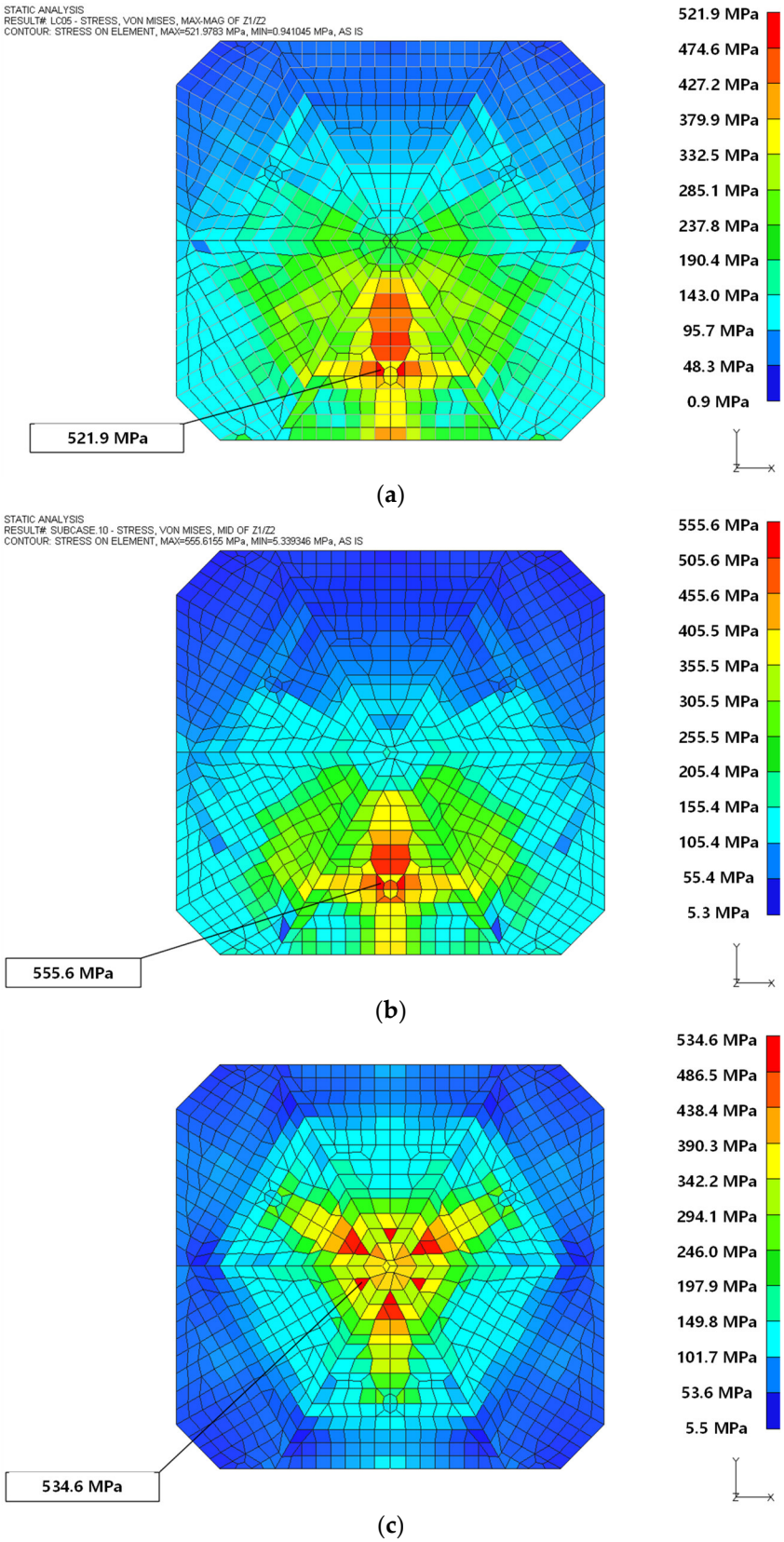

Figure 15. The von Mises stress distribution of the bottom plane: (**a**) LC06 (existing procedure); (**b**) LC06 (newly proposed procedure); (**c**) LC07 (newly proposed procedure).

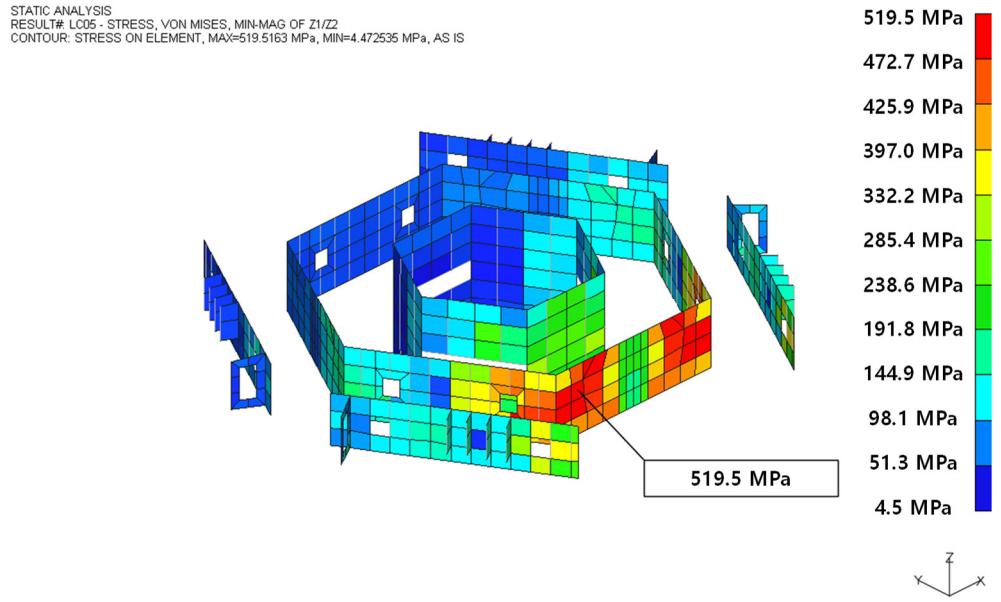

(**a**)

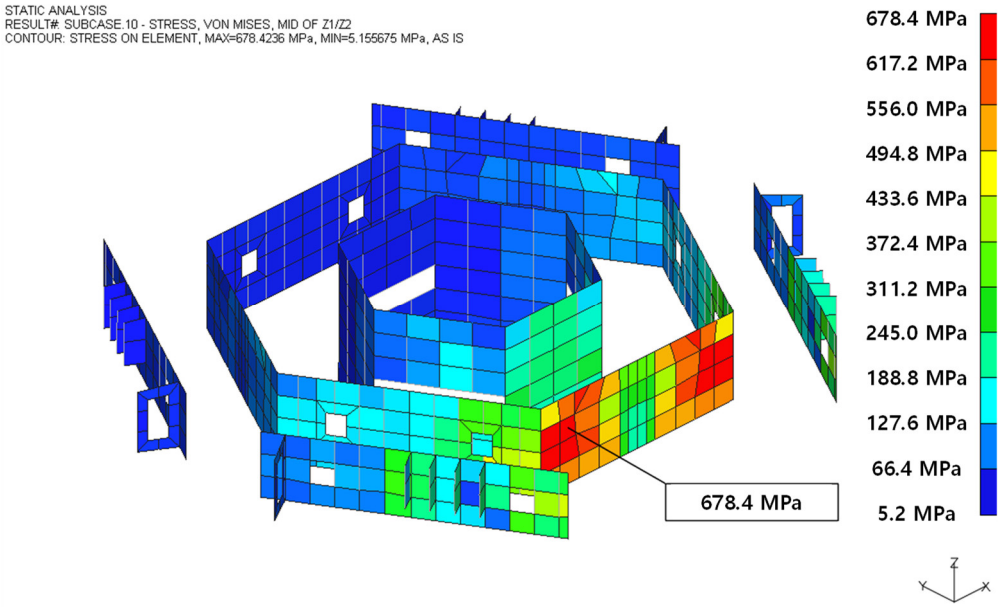

(**b**)

Figure 16. The von Mises stress distribution of LNO 4, 9, and 15: (**a**) LC06 (existing procedure); (**b**) LC06 (newly proposed procedure).

3.4.2. Buckling Assessment

In this study, a buckling assessment of the spudcan was conducted based on the ABS buckling criteria [15]. Buckling safety was evaluated using maximum allowable strength utilization factors (η), which are the inverse of safety factors. For a loading condition that is characterized as static loading

$$\eta = 0.60$$

For a loading condition that is characterized as a combined loading or severe storm condition

$$\eta = 0.80$$

Table 8 shows the results of the buckling panel check, and Figures 16–18 show the utilization factor of each analysis case.

Table 8. Results of the buckling panel check.

Location	Allowable Utilization Factor	Utilization Factor	
		Static Loading	Combined Loading
Top plane	<0.6 for static <0.8 for combined	0.12	0.48
Bottom plane		0.26	0.68
Side shell		0.07	0.53
Main support		0.23	0.50
Sub support		0.20	0.51
LNO 4		0.28	0.59
LNO 9		0.10	0.49
LNO 13		0.08	0.58

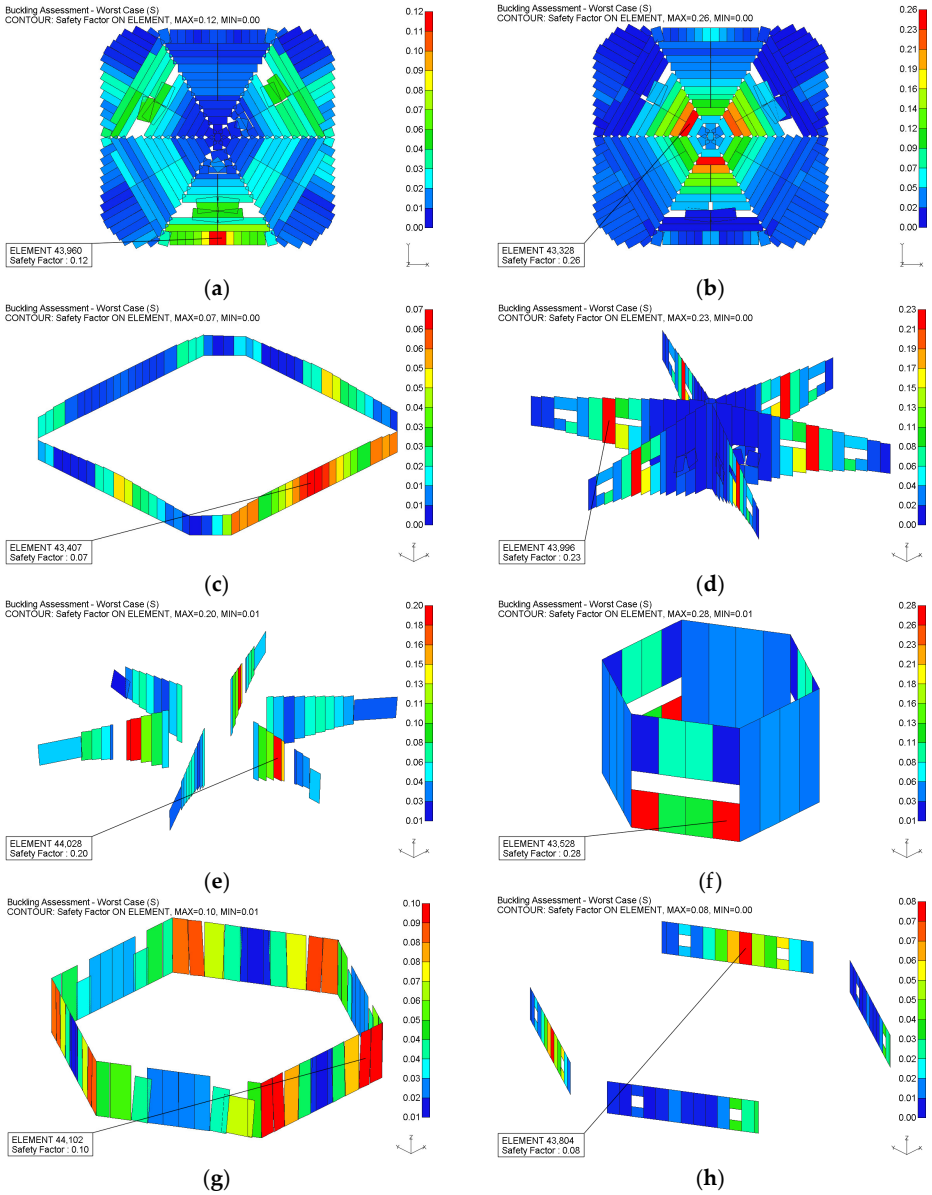

Figure 17. Buckling panel check for static loading: (**a**) top plane; (**b**) bottom plane; (**c**) side shell; (**d**) main support; (**e**) sub support; (**f**) LN04; (**g**) LN09; (**h**) LN13.

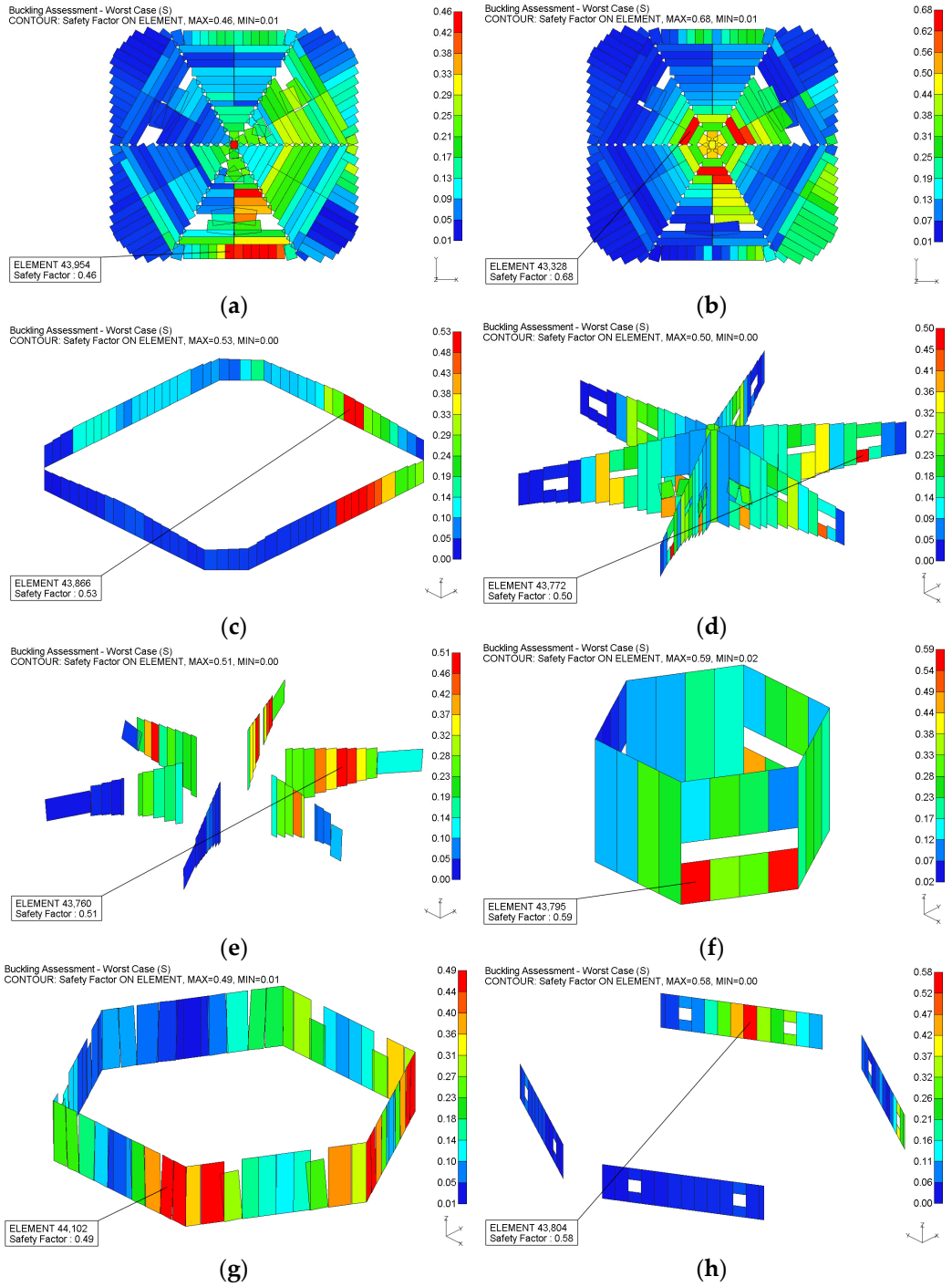

Figure 18. Buckling panel check for combined loading: (**a**) top plane; (**b**) bottom plane; (**c**) side shell; (**d**) main support; (**e**) sub support; (**f**) LN04; (**g**) LN09; (**h**) LN13.

3.4.3. Structure Design

Table 9 presents information on the weight and maximum and minimum plate thickness for each section of the spudcan structure. The overall weight increased by approximately 9.8%, with a weight increase of approximately 60% in the main support and 42% in the side shell. Figure 19 shows the thickness plot of the main support of the spudcan designed by the existing and the proposed procedures. This weight increase is likely due to the addition of the lateral impact loading conditions, which can be caused by the difference in slope between the spudcan and the seabed and the increased pressure on the outer perimeter as the soil bearing capacity by the ground is reduced. Despite the presence of local load

conditions in the bottom surface, the weight of the bottom surface actually decreased, which suggests that the major structural members contribute significantly to the localized strength of the bottom plate members. In addition, the thickness of the outer plate did not change under lateral loading conditions, which is likely due to the radially densely spaced outer ribs. As a result, the reinforcement of the main support and the side shell, which account for a relatively small portion of the total weight, satisfy the additional loading conditions, leading to an overall weight increase of only 9.8%. This underscores the importance of the presence of outer ribs as a critical design factor in spudcan structure design.

Table 9. The result of weight and thickness by comparing existing the design procedures and the newly proposed design procedure.

Location	Existing Design Procedure			Newly Proposed Design Procedure			B/A
	Weight, A (ton)	Max. Plate Thickness (mm)	Min. Plate Thickness (mm)	Weight, B (ton)	Max. Plate Thickness (mm)	Min. Plate Thickness (mm)	
Top plane	66.51	50.0	30.0	67.08	50.0	30.0	1.009
Bottom plane	62.38	50.0	30.0	59.40	60.0	30.0	0.952
Side shell	18.29	30.0	30.0	26.03	50.0	30.0	1.423
Main support	31.71	50.0	20.0	50.75	60.0	40.0	1.600
Sub support	30.66	80.0	20.0	29.29	80.0	20.0	0.955
LNO 4	12.74	40.0	20.0	15.33	50.0	25.0	1.203
LNO 9	27.78	190.0	20.0	26.35	190.0	20.0	0.948
LNO 13	10.89	30.0	15.0	12.31	35.0	15.0	1.130
Total	260.96	-	-	286.55	-	-	1.098

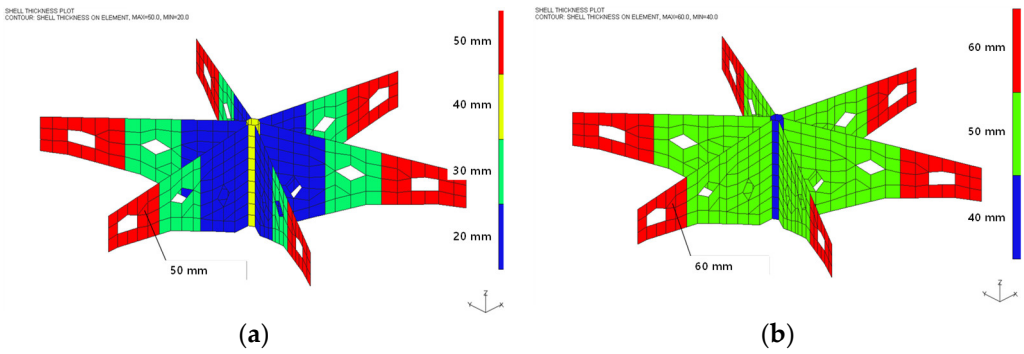

Figure 19. Thickness plot of the main support: (**a**) existing design procedure; (**b**) newly proposed design procedure.

4. Conclusions

The existing procedure for evaluating the strength of spudcan structures has not been specified by classification societies, and some of the conditions mentioned are also vague, which has led to a lot of disagreement about the procedure. In this study, the design load conditions were supplemented to refine and improve the existing spudcan structural strength evaluation procedure, and accordingly, it was confirmed how it affects the spudcan structural design. The additional load conditions proposed in the new procedures may occur during actual WTIV operation. Therefore, there is a need to revise the classification regulations by revising and supplementing the current procedures.

The modified and added design load conditions required an increase in structural weight of approximately 9.8% but should provide structural stability under design load conditions that are reasonably likely to occur. In addition, there are other potential conditions, such as loads acting on a protruding spudcan during operation and collision with the seabed due to vessel motions during installation work, but considering the size and shape

of the loads, it was determined that the structural strength assessment procedure presented in this study can be covered. The proposed spudcan structure evaluation procedure will be applied to real projects, but there is still plenty of room for improvement. Future studies should continue to enhance the evaluation procedure by identifying and modifying new design load conditions.

Author Contributions: Conceptualization, J.-S.P.; methodology, J.-S.P. and M.-S.Y.; data curation, M.-S.Y. and D.-H.L.; writing—original draft preparation, J.-S.P. and D.-H.L.; writing—review and editing, M.-S.Y. All authors have read and agreed to the published version of the manuscript.

Funding: This research was supported by the Basic Science Research Program through the National Research Foundation of Korea (NRF) funded by the Ministry of Education (MOE) (NRF-2022R1I1A3068558).

Data Availability Statement: The data are not publicly available. The data presented in this study are available on request from the corresponding author.

Conflicts of Interest: The authors declare no conflict of interest.

References

1. Global Wind Energy Council (GWEC). World Energy Outlook 2020, Flagship Report, Chapter 14. In *Outlook for Offshore Wind*; Global Wind Energy Council: Brussels, Belgium, 2020; pp. 613–620.
2. Osborne, J.J.; Houlsby, G.T.; The, K.L.; Leung, C.F.; Bienen, B.; Cassidy, M.J.; Randolph, M.F. Improved Guidelines for the Prediction of Geotechnical Performance of Spudcan Foundations during Installation and Removal of Jack-up Units. In Proceedings of the Offshore Technology Conference (OTC 20291), Houston, TX, USA, 4–7 May 2009; pp. 1–20.
3. Puyang, Z.; Xiaoyang, Y.; Hongyan, D. Spudcan Bearing Capacity Calculation of the Offshore Jack-up Drilling Platform during the Preloading Process. *Pet. Explor. Dev.* **2011**, *38*, 613–619.
4. Cho, T.M.; Park, J.S.; Ha, Y.S.; Kim, B.J.; Jang, K.B. Global In-Place Analysis of WTIV Leg for Korean West-South Offshore Wind Zone. In Proceedings of the Twenty-Fourth ISOPE Conference, Busan, Republic of Korea, 15–20 June 2014; pp. 376–382.
5. Fonseca, E.M.M.; Melo, F.J.M.Q. Numerical Solution of Curved Pipes submitted to in-plane Loading Conditions. *Thin-Walled Struct.* **2010**, *48*, 103–109. [CrossRef]
6. Jin, H.B.; Jang, B.S.; Choi, J.H.; Zhao, J.; Kang, S.W. Comparison of Analysis Methods for Designed Spudcan Bearing Capacity and Penetration Behavior for Southwest Sea Soil. *J. Ocean. Eng. Technol.* **2015**, *29*, 175–185. [CrossRef]
7. Park, J.S.; Ha, Y.S.; Jang, K.B.; Radha. Structure & Installation engineering for offshore jack-up rigs. *J. Nav. Archit.* **2017**, *54*, 39–46.
8. Society of Naval Architects and Marine Engineers (SNAME). *Guidelines for Site Specific Assessment of Mobile Jack-Up Units*; Technical & Research Bulletin 5-5a; SNAME: Alexandria, VA, USA, 2002.
9. Yu, L.; Zang, H.; Li, J.; Wang, X. Finite Element Analysis and Parametric Study of Spudcan Footing Geometries Penetrating Clay Near Existing Footprints. *J. Mar. Sci. Eng.* **2019**, *7*, 175. [CrossRef]
10. Yu, H.; Sun, Z.; He, L.; Yang, L. Research on Optimal Design of Spudcan Structures to Ease Spudcan-Footprint Interactions in Clay and Comparative Analyses with Different Measures. *J. Pol. Marit. Res.* **2022**, *29*, 43–56. [CrossRef]
11. Cassidy, M.J.; Vlahos, G.; Hodder, M. Assessing Appropriate Stiffness Levels for Spudcan Foundations on Dense Sand. *Mar. Struct.* **2010**, *23*, 187–208. [CrossRef]
12. *DNV-OS-C201*; Structural Design of Offshore Units (WSD Method)-Offshore Standard DNV-OS-C201, Chapter 2, Section 11; Recommended Practice. Det Norske Veritas (DNV): Oslo, Norway, 2008.
13. HEXAGON. Chapter 6, Material Modeling. In *Patran 2016-User's Guide*; HEXAGON: Torrance, CA, USA, 2016; pp. 124–131.
14. *DNV-OS-C101*; Design of Offshore Steel Structures, General (LRFD Method)-Offshore Standard. Section 3. Det Norske Veritas (DNV): Oslo, Norway, 2011.
15. American Bureau of Shipping (ABS). Rules for Building and Classing Mobile Offshore Units. In *Recommended Practice*; ABS: Houston, TX, USA, 2021.

Disclaimer/Publisher's Note: The statements, opinions and data contained in all publications are solely those of the individual author(s) and contributor(s) and not of MDPI and/or the editor(s). MDPI and/or the editor(s) disclaim responsibility for any injury to people or property resulting from any ideas, methods, instructions or products referred to in the content.